Available online at www.sciencedirect.com
SCIENCE DIRECT®
Journal of Solid State Chemistry 178 (2005) 621–628
JOURNAL OF SOLID STATE CHEMISTRY
www.elsevier.com/locate/jssc

Synthesis and structural characterization of a new open-framework zinc terephthalate $Zn_3(OH)_2(bdc)_2 \cdot 2DEF$, with infinite Zn–($\mu_3$-OH)–Zn chains

Thierry Loiseau[a,*], Hervé Muguerra[a], Gérard Férey[a,b], Mohamed Haouas[a], Francis Taulelle[a]

[a]*Institut Lavoisier (UMR CNRS 8637), Université de Versailles St Quentin en Yvelines, 45, Avenue des Etats Unis, FR-78035 Versailles Cedex, France*
[b]*Institut Universitaire de France, Université de Versailles St Quentin en Yvelines, 45, Avenue des Etats Unis, 78035 Versailles, France*

Received 20 October 2004; received in revised form 29 November 2004; accepted 2 December 2004

Abstract

A new zinc carboxylate $Zn_3(OH)_2(bdc)_2 \cdot 2DEF$ was synthesized under mild hydrothermal conditions (100 °C, 40 h) in the presence of 1,4-benzenedicarboxylic (bdc) acid, in *N,N′*-diethylformamide (DEF) solvent. Its structure, characterized by means of single-crystal XRD analysis, consists of connection of $ZnO_2(OH)_2$ tetrahedra corner-sharing with $ZnO_4(OH)_2$ octahedra. Two adjacent $ZnO_2(OH)_2$ tetrahedra have a common edge corresponding to hydroxy group, which is also linked to the octahedrally coordinated zinc atoms with a μ_3 configuration. This resulting connection mode generates infinite chains running along the *c*-axis, and connected to each other via the bdc ligand. Three-dimensional framework is therefore formed with channels running along the *c*-axis, parallel to the infinite Zn–OH–Zn chains. Within the tunnels are trapped the DEF species, which interacts via hydrogen-bond to the μ_3-hydroxy of the zinc chains with the terminal oxygen atom of the formamide function. Analysis by solid state NMR (^{1}H and ^{13}C) has confirmed both the presence of occluded solvent molecules within the pores and the incorporation of carboxylate moieties into the framework. The structure of $Zn_3(OH)_2(bdc)_2 \cdot 2DEF$ is closely related to those of MOF-69 series, constructed with longer organic linkers (4,4′-biphenyldicarboxylate and 2,6-naphthalenedicarboxylate). The structure is observed to loose crystallinity upon heating and removal of the occluded DEF moieties.

Crystal data for $[Zn_9(OH)_6(O_2C–C_6H_4–CO_2)_6] \cdot 6[(CH_3–CH_2)_2NCHO]$: $a = 17.7374(3)$ Å, $b = 15.2605(2)$ Å, $c = 18.2635(2)$ Å, $\beta = 113.071(1)°$, $V = 4548.2(1)$ Å^3, $P2_1/n$ (no. 14), $Z = 1$, $R_1 = 0.0510$, $wR_2 = 0.1302$ for 11877 reflections $I > 2\sigma(I)$.

Keywords: Hydrothermal synthesis; Zinc; 1,4-benzenedicarboxylic acid; Metal-organic frameworks; XRD crystal structure; Solid state NMR; ^{1}H; ^{13}C

1. Introduction

The construction of the metal-organic frameworks (MOFs) has currently attracted attention since this emerging new class of porous solids exhibits molecular adsorption and storage properties similar to those found in the zeolites materials [1–8]. These compounds are usually built up from discrete metal oxide clusters linked to each other through rigid organic ligands such as aromatic poly-carboxylates or -amines. The resulting coordination polymers possess various interesting three-dimensional topologies depending on the diversity of the connection modes of the multifunctional benzene-based species and the point symmetry of metal–oxygen or metal–nitrogen cores (tetrahedral, octahedral, etc.). In other structures, the metal–oxygen building blocks consists of infinite chains connected via the organic linkers and this gives rise to the formation of one-dimensional channel networks [9–14]. In some cases,

*Corresponding author. Fax: +33 1 39 254 358.
E-mail address: loiseau@chimie.uvsq.fr (T. Loiseau).

0022-4596/$ - see front matter © 2005 Elsevier Inc. All rights reserved.
doi:10.1016/j.jssc.2004.12.004

their mixed porous organic–inorganic frameworks are stable enough to be employed for applications in the field of gas adsorption [15]. For instance, some materials were found to be very efficient for the hydrogen adsorption [16–19].

In order to investigate several gas adsorption properties of the zinc carboxylate MOF-5 [20] material, we attempted to synthesize it from the procedure described in reference [21] by Yaghi et al. It was reported that large scale preparation of the MOF-5 compound could be carried out from a mixture of zinc nitrate, 1,4-benzenedicarboxylic acid (called terephthalic acid) and *N,N′*-diethylformamide (DEF) as solvent, heated at 85–105 °C in a closed cell. However, with these conditions, we were unable to obtain the MOF-5 phase but another compound crystallizes when the synthesis is performed under autogenous pressure at 100 °C in an autoclave. The present work deals with the preparation and crystal structure characterization of the new solid, $Zn_3(OH)_2(bdc)_2 \cdot 2DEF$ (bdc = 1,4-benzenedicarboxylate; DEF = *N,N′*-diethylformamide). Its XRD single-crystal and thermogravimetric analyses, and ^{13}C, ^{1}H NMR are presented. Its three-dimensional structure is close to that of the zinc carboxylates MOF-69 [11] series, previously reported by Yaghi et al.

2. Experimental

2.1. Synthesis

The zinc terephthalate $Zn_3(OH)_2(bdc)_2 \cdot 2DEF$ was hydrothermally synthesized under autogeneous pressure using a solution of DEF as solvent, in the presence of 1,4-benzenedicarboxylic acid. The starting reactants were zinc nitrate ($Zn(NO_3)_3 \cdot 6H_2O$, Aldrich, 98%), 1,4-benzenedicarboxylic acid ($C_6H_4(CO_2H)_2$, Acros Organics, 99%) and *N,N′*-diethylformamide ($(CH_3–CH_2)_2NCHO$, Interchim, 99%). Typically, the reaction mixture containing the molar ratio 1.4 Zn (0.875 mmol, 0.2602 g), 0.7 bdc (0.4375 mmol, 0.0727 g), 80 DEF (50 mmol, 5 ml) was placed in a 23 ml Teflon-lined steel Parr autoclave at 100 °C for 40 h. The pH of synthesis was 4. A white powdered product (yield: 72%) was filtered off, washed with deionized water and dried in air at room temperature. Scanning electron microscope examination indicated (Fig. 1) that the sample is composed of prismatic needle-like crystals of 200–300 μm size. Preliminary X-ray powder diffraction pattern showed it to be a novel phase.

2.2. Single crystal X-ray structure analysis

A colorless needle-shape crystal ($0.28 \times 0.16 \times 0.12\,mm^3$) of $Zn_3(OH)_2(bdc)_2 \cdot 2DEF$ was selected under polarizing optical microscope and glued on a glass fiber for a single-crystal X-ray diffraction experiment. The intensity data were recorded on a Siemens SMART three-circle diffractometer equipped with a CCD bidimensional detector (molybdenum radiation). The crystal-to-detector distance was 45 mm allowing for the data collection up to 60° (2θ). Slightly more than one hemisphere of data was recorded and the acquisition time per frame was 30 s with a scan width of 0.3° in ω. An empirical absorption correction was applied using the SADABS [22] program. The structure of $Zn_3(OH)_2(bdc)_2 \cdot 2DEF$ was solved by direct methods in the centric space group $P2_1/n$ (no. 14) and refined by full-matrix least squares using the SHELXTL [23] package on the basis of F^2. The five unique zinc atoms were first revealed and the remaining atoms (O, C, N) were placed from successive Fourier maps analyses. The hydrogen atoms were placed using geometrical constraints (HFIX card). It also includes additional hydrogen atoms bonded to the oxygen atoms bridging the zinc atoms (μ_3-hydroxy configuration). The final refinement including anisotropic thermal parameters of all non-hydrogen atoms converged to $R_1 = 0.0510$ and $wR_2 = 0.1302$. The chemical formula of the title compound deduced from the XRD analysis is $[Zn_3(OH)_2(O_2C–C_6H_4–CO_2)_2] \cdot 2[(CH_3–CH_2)_2NCHO]$. The crystal data are given in Table 1. The coordinates of non-hydrogen atoms are listed in Table 2.

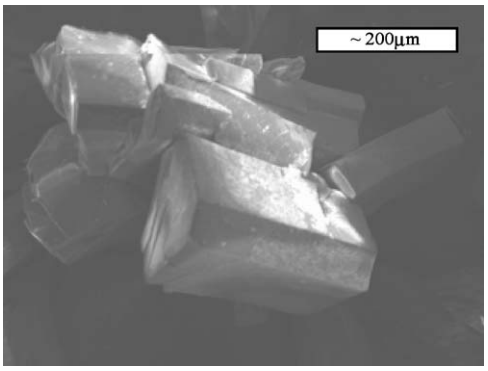

Fig. 1. Scanning Electron Microscopy photograph of crystals of $Zn_3(OH)_2(bdc)_2 \cdot 2DEF$.

2.3. Solid-state NMR spectroscopy

Solid-state ^{13}C and ^{1}H NMR characterizations were performed on a Bruker Avance500 spectrometer with an 11.7 T magnetic field, in which these nuclei resonate at 125.8 and 500.1 MHz, respectively. An H/X 4 mm MAS probehead and a classical ZrO_2 rotor spun at 12.5 kHz were used for ^{13}C experiments. For the acquisition of ^{1}H MAS spectra, the spinning rate was 30 kHz using 2.5 mm rotor. The RF field frequency, pulse duration, number of scans, and repetition time were 60 kHz, 2.1 μs, 80 scans, and 2 s for ^{1}H MAS spectra, and

Table 1
Crystal data and structure refinement for $Zn_3(OH)_2(bdc)_2 \cdot 2DEF$

Chemical formula	$Zn_9(OH)_6(O_2C–C_6H_4–CO_2)_6 \cdot 6((CH_3–CH_2)_2NCHO)$
Empirical formula	$C_{156}H_{192}N_{12}O_{72}Zn_{18}$
Formula weight	4563.88
Temperature	293(2) K
Wavelength	0.71073 Å
Crystal system, space group	Monoclinic, $P2_1/n$
Unit cell dimensions	$a = 17.7374(3)$ Å.
	$b = 15.2605(2)$ Å, $\beta = 113.071(1)^\circ$.
	$c = 18.2635(2)$ Å.
Volume	4548.20(11) Å^3
Z, Calculated density	1, 1.666 Mg/m^3
Absorption coefficient	2.418 mm^{-1}
$F(000)$	2328
Crystal size	0.28 × 0.16 × 0.12 mm
Theta range for data collection	1.36–29.83°.
Limiting indices	$-24 \leqslant h \leqslant 16$, $-17 \leqslant k \leqslant 20$, $-25 \leqslant h \leqslant 24$
Reflections collected/unique	30994/11877 (R(int) = 0.0356)
Completeness to $\theta = 29.83$	91.0%
Absorption correction	Sadabs
Refinement method	Full-matrix least-squares on F^2
Data/parameters	11877/485
Goodness-of-fit on F^2	1.008
Final R indices [$I > 2\sigma(I)$]	$R_1 = 0.0510$, $wR_2 = 0.1302$
R indices (all data)	$R_1 = 0.1335$, $wR_2 = 0.1710$
Extinction coefficient	0.00017(6)
Largest diff. peak and hole	0.767 and −0.710 eÅ^{-3}

Table 2
Atomic coordinates (× 10^4) and equivalent isotropic displacement parameters (Å^2 × 10^3) for $Zn_3(OH)_2(bdc)_2 \cdot 2DEF$. U(eq) is defined as one third of the trace of the orthogonalized U_{ij} tensor

	x	y	z	U(eq)
Zn(1)	0	0	0	22(1)
Zn(2)	−3(1)	−46(1)	−3342(1)	22(1)
Zn(3)	−20(1)	−964(1)	−1662(1)	25(1)
Zn(4)	23(1)	960(1)	−4952(1)	24(1)
Zn(5)	20(1)	932(1)	−1671(1)	24(1)
O(1)	471(2)	−35(2)	−2113(2)	24(1)
O(2)	−476(2)	−18(2)	−4567(2)	22(1)
O(3)	−470(2)	13(2)	−1221(2)	23(1)
O(4)	−834(2)	−1697(2)	−2422(2)	37(1)
O(5)	767(2)	−1723(2)	−900(2)	38(1)
O(6)	−758(2)	1765(2)	−5681(2)	35(1)
O(7)	1118(2)	538(2)	−3254(2)	34(1)
O(8)	−1083(2)	−677(2)	−3365(2)	34(1)
O(9)	653(2)	1203(2)	109(2)	40(1)
O(10)	916(2)	1587(2)	−4161(2)	36(1)
O(11)	1042(2)	−693(2)	36(2)	36(1)
O(12)	531(2)	−1294(2)	−3271(2)	38(1)
O(13)	−574(2)	1207(2)	−3464(2)	39(1)
O(14)	906(2)	1615(2)	−943(2)	42(1)
O(15)	−851(2)	1615(2)	−2424(2)	40(1)
C(1)	−905(3)	1751(3)	−6422(2)	28(1)
C(2)	−1576(3)	2337(3)	−6952(2)	30(1)
C(3)	3090(3)	2821(3)	−2767(2)	34(1)
C(4)	2417(3)	2359(3)	−3261(2)	37(1)
C(5)	2071(3)	1708(3)	−2956(2)	31(1)
C(6)	1312(3)	1239(3)	−3489(2)	28(1)
C(7)	2427(3)	1515(3)	−2149(2)	39(1)
C(8)	3094(3)	2000(3)	−1649(2)	38(1)
C(9)	1166(3)	−1417(3)	−212(2)	31(1)

Table 2 (*continued*)

	x	*y*	*z*	*U*(eq)
C(10)	1843(3)	−1985(3)	327(2)	32(1)
C(11)	2297(3)	−1722(3)	1109(2)	39(1)
C(12)	−2071(3)	−2758(3)	−3391(2)	39(1)
C(13)	−1893(3)	−1966(3)	−3666(2)	33(1)
C(14)	−1214(3)	−1400(3)	−3119(2)	30(1)
C(15)	−2331(3)	−1705(3)	−4444(2)	40(1)
C(16)	2033(3)	−2771(3)	54(2)	38(1)
C(17)	−996(3)	1592(3)	−3165(2)	29(1)
C(18)	−1758(3)	2071(3)	−3695(2)	31(1)
C(19)	−1987(3)	2059(3)	−4514(2)	39(1)
C(20)	2299(3)	2519(3)	2(2)	40(1)
C(21)	1815(3)	2078(3)	322(2)	29(1)
C(22)	1063(3)	1589(3)	−198(2)	30(1)
C(23)	2055(3)	2063(3)	1146(2)	35(1)
C(24)	−2239(3)	2514(3)	−3368(2)	36(1)
O(1N1)	2151(2)	−299(2)	−1210(2)	56(1)
C(1N1)	2454(4)	−44(3)	−529(3)	49(1)
N(2N1)	3205(3)	−215(3)	−13(3)	60(1)
C(2N1)	3792(4)	−688(4)	−268(4)	79(2)
C(3N1)	4195(5)	−1414(5)	254(4)	110(3)
C(4N1)	3494(5)	168(5)	787(4)	88(2)
C(5N1)	4132(5)	819(5)	929(5)	110(3)
O(1N2)	−2174(3)	16(2)	−5477(3)	62(1)
C(1N2)	2466(4)	−354(4)	−3864(3)	59(2)
N(1N2)	3244(3)	−332(3)	−3372(3)	62(1)
C(2N2)	3837(5)	181(4)	−3563(4)	79(2)
C(3N2)	4267(5)	841(5)	−2966(4)	102(2)
C(4N2)	3537(5)	−837(5)	−2613(4)	94(2)
C(5N2)	4050(5)	−1600(5)	−2627(5)	116(3)
O(3N3)	−2162(2)	−162(2)	−2084(2)	56(1)
C(1N3)	−2459(4)	96(3)	−2766(3)	53(2)
N(1N3)	−3209(3)	−68(3)	−3282(3)	61(1)
C(2N3)	−3768(4)	−604(4)	−3067(4)	68(2)
C(3N3)	−4070(4)	−1376(4)	−3581(4)	84(2)
C(4N3)	−3504(6)	315(5)	−4095(5)	105(3)
C(5N3)	−4173(6)	940(6)	−4227(5)	134(3)

42 kHz, 5.9 μs, 512 scans, and 10 s for $^{13}C\{^{1}H\}$ MAS spectra with broadband decoupling. Chemical shift reference is TMS for ^{1}H and ^{13}C.

3. Results and discussion

3.1. Structure description

The structure of $Zn_3(OH)_2(bdc)_2 \cdot DEF$ exhibits a three-dimensional framework consisting of infinite one-dimensional chains of zinc oxyhydroxide $[Zn_3O_8(OH)_2]_n$ connected to each other through the 1,4-benzenedicarboxylate (bdc) ligands. The asymmetric unit of the $[Zn_3O_8(OH)_2]_n$ chains is composed of five crystallographically zinc sites (Fig. 2). Two of them (Zn1 and Zn2) are octahedrally coordinated to four oxygen atoms belonging to the carboxylate ligand of the bdc species and two oxygen atoms corresponding to hydroxyl group OH. The Zn–O distances range from 2.107(3) to 2.138(3) Å whereas the Zn–OH ones are slightly shorter (2.053(3)–2.066(3) Å). The hydroxyl groups are located in *trans* position within the octahedral $ZnO_4(OH)_2$ units. The three other crystallographically zinc atoms are in tetrahedral coordination with two oxygen atoms of carboxylate ligand and two other corresponding to hydroxyl groups. In contrast with the octahedral entities, the Zn–O distances (1.921(3)–1.937(3) Å) are shorter than the Zn–OH ones (1.988(3)–2.010(3) Å). The tetrahedral units are linked to each other via an edge with two hydroxyl groups, which are also bonded to the octahedral zinc atoms. It results in the formation of an original straight chain $[Zn_3O_8(OH)_2]_n$ (Fig. 2) of $ZnO_4(OH)_2$ octahedra strictly alternating with the bi-tetrahedral units $Zn_2O_4(OH)_2$. The three crystallographically unique OH groups (O1, O2 and O3) have a μ_3-hydroxy bridging configuration. The occurrence of such hydroxyl moieties is in good agreement with bond valence calculations [24] for the corresponding oxygen atoms with values of 1.3, 1.28 and 1.27 for O1, O2 and O3, respectively (a theoretical value of 1.2 is expected for OH). This is also confirmed from the examination of

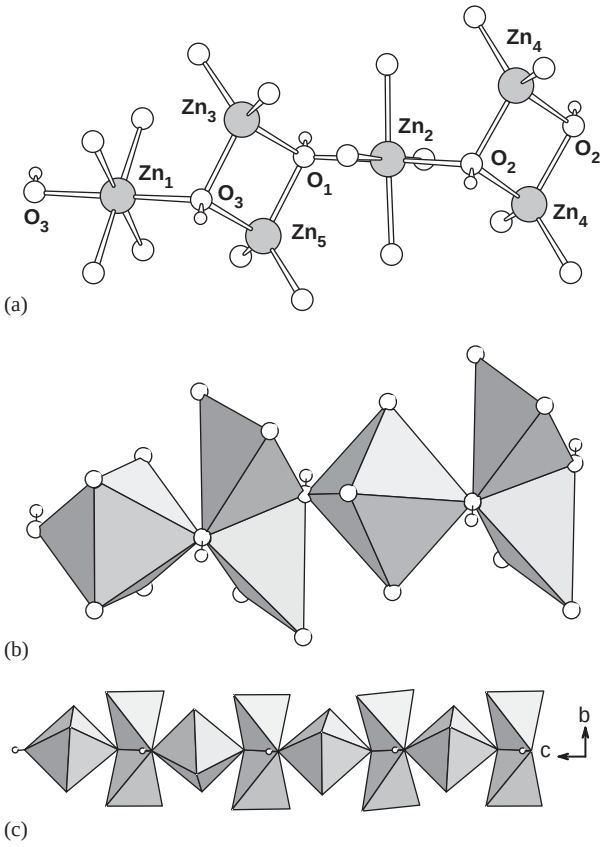

Fig. 2. Asymmetric unit (ball and stick (a) and polyhedra (b)) in $Zn_3(OH)_2(bdc)_2 \cdot 2DEF$, showing the edge-sharing bi-tetrahedral unit $ZnO_2(OH)_2$ and octahedral unit $ZnO_4(OH)_2$. (c) Polyhedral representation of one infinite chains of $[Zn_3O_8(OH)_2]_n$ running along the *c*-axis.

the Zn–OH–Zn angles, which are consistent with the expected tetrahedral surrounding (92.8(1)–113.5(1)°) for such a μ_3-hydroxy configuration. The presence of a μ_3-oxo group would rather induce a trigonal plane with Zn–O–Zn angles close to 120° [25]. Similar situations were previously reported in other zinc carboxylates [26–28], in which discrete clusters of Zn(μ_3-OH) cores are found. For instance, the structure of the zinc crotonate [28] ($Zn_5(OH)_2(O_2CHCHCH_3)_8$) is built up from isolated molecular building block comprising one central octahedrally coordinated zinc linked through OH groups to two tetrahedrally coordinated zinc atoms. However, in the latter, the tetrahedral units only share a corner via the μ_3-hydroxy group (not an edge).

The infinite $[Zn_3O_8(OH)_2]_n$ chains parallel to the *c*-axis are linked to each other through the bdc moieties (Fig. 3). The carboxylate ion of the bdc species, $R\text{-}CO_2^-$, acts as a bridging bidentate ligand adopting an usual *syn-syn* configuration [29,30]. The two oxygen atoms of each carboxylic acid function are linked to two consecutive zinc atoms having two different coordination spheres (tetrahedron and octahedron). The connection of the infinite $[Zn_3O_8(OH)_2]_n$ chains and bdc occurs along the two perpendicular directions [110] and [1 $\bar{1}$ 0]

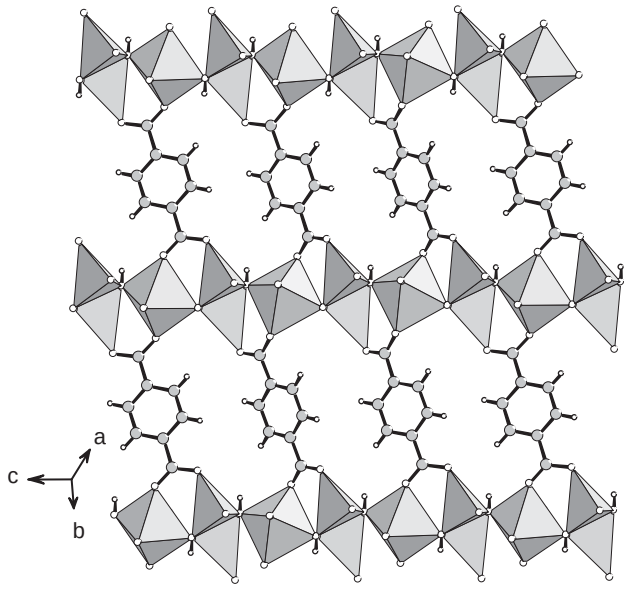

Fig. 3. View of the structure of $Zn_3(OH)_2(bdc)_2 \cdot 2DEF$, showing the connection of the 1,4-benzenedicarboyxylate ligands with the infinite chains running along the *c*-axis (gray polyhedra: $ZnO_2(OH)_2$ and $ZnO_4(OH)_2$).

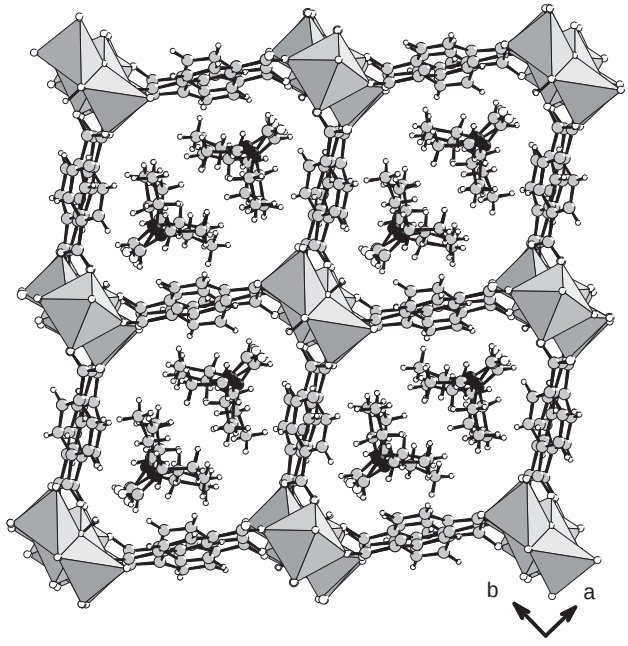

Fig. 4. Representation of the three-dimensional framework of $Zn_3(OH)_2(bdc)_2 \cdot 2DEF$ along the *c*-axis, with the occluded DEF molecules within the channels (gray polyhedra: $ZnO_2(OH)_2$ and $ZnO_4(OH)_2$).

in order to generate a mixed organic–inorganic three-dimensional network delimiting rhombic channels running along the *c*-axis, parallel to the inorganic zinc-based chains (Fig. 4). The free tunnel size was estimated to be 8.3×10.1 Å (it was taken into account the oxygen ionic radius of 1.35 Å). Three crystallographically unique DEF molecules are trapped within the channels.

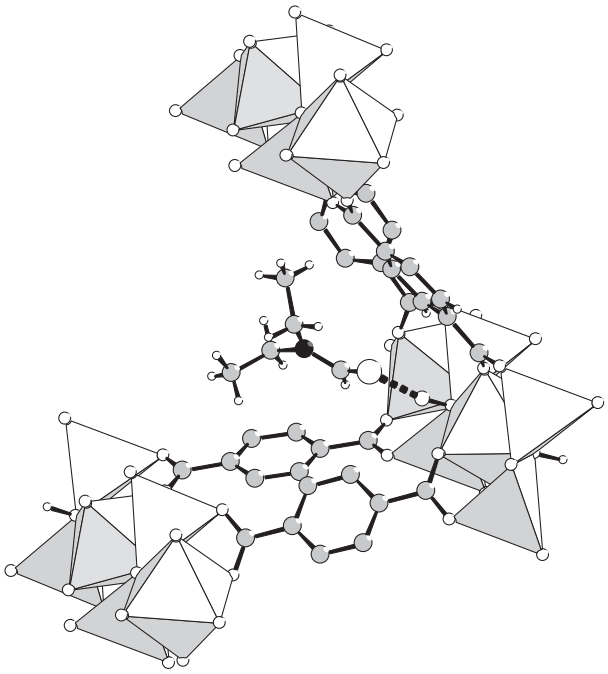

Fig. 5. Details of the hydrogen bond interaction between the oxygen atoms of the formamide group of the occluded DEF molecule and the hydrogen atom of the μ_3-hydroxy group. (white and light gray polyhedra: $ZnO_2(OH)_2$ and $ZnO_4(OH)_2$, gray circles: C, black circle: N, large open circles: O, small open circles: H, hydrogen atoms of benzene ring have been omitted for clarity).

The ethyl groups are pointing towards the center of the structural pores space whereas the oxygen atoms of the formamide function preferentially interacts with the μ_3-hydroxy groups bridging the zinc atoms through hydrogen bond (N–HC = O···HO) (Fig. 5). The strong hydrogen bond interactions are revealed by the occurrence of short –C = O···H–O distances between the three distinct occluded organic species and OH groups (O3N3···H3 = 1.847 Å, O2N2···H2 = 1.854 Å and O1N1···H1 = 1.863 Å).

The structure of $Zn_3(OH)_2(bdc)_2 \cdot DEF$ is closely related to those of the MOF-69 series, recently reported by Yaghi et al. [11]. These solids were synthesized at room temperature (7 days) by using 4,4′-biphenyldicarboxylic (= $bpdcH_2$, $Zn_3(OH)_2(bpdc)_2 \cdot 4DEF \cdot 2H_2O$, MOF-69A) and 2,6-naphthalenedicarboxylic acids (= $ndcH_2$, $Zn_3(OH)_2(ndc)_2 \cdot 4DEF \cdot 2H_2O$, MOF-69B) as rigid linkers. Their structures described from the expansion of the $SrAl_2$-type net [31], are identical and built up from the similar infinite chains of $[Zn_3O_8(OH)_2]_n$ linked together by the bpdc or ndc ligands. Only the channel size differs between the compounds because of the length of the rigid organic spacer. Larger pores are observed in the MOF-69 compounds (13.0 × 16.7 Å for MOF-69A and 10.7 × 14.6 Å for MOF-69B), constructed with aromatic linkers comprising two benzene rings. Our phase is the third example of zinc carboxylate consisting of such infinite Zn–O–Zn chains based on the connection of octahedral and bi-tetrahedral building blocks.

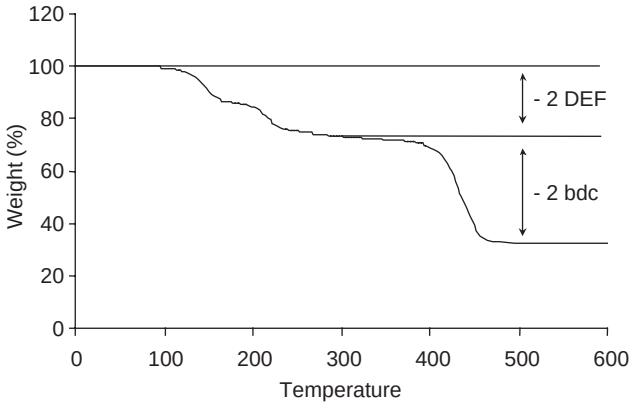

Fig. 6. TG curve of $Zn_3(OH)_2(bdc)_2 \cdot DEF$ (under N_2, heating rate 3 °C min^{-1})

3.2. Solid state NMR

$Zn_3(OH)_2(bdc)_2 \cdot 2DEF$ was subjected to ^1H and $^{13}C\{^1H\}$ decoupled NMR measurements. The ^1H NMR spectrum is displayed in Fig. 7 and is comprised of at least six overlapping signals. The shielded signal at $\delta = -0.4$ ppm can be assigned to the Zn–OH–$(Zn)_2$ μ_3-bridging hydroxides. The three lines at $\delta = 1.6$, 3.0 and 7.7 ppm with relative intensities of 6:4:1 are attributable respectively to the methyl, methylene and aldehyde functions of DEF molecule. Two components in the aromatic resonance region are featured at $\delta = 7.0$ and 8.4 ppm that could account for two different environment of terephthalate moieties (bdc) in the solid. There is no trace of any unshielded signal at around $\delta =$ 12.5 ppm of acidic proton (COOH) [13] indicating that the carboxylic acid is deprotonated as expected. Fig. 8 displays the $^{13}C\{^1H\}$ decoupled NMR spectrum. The signals at $\delta = 9.5$, 13.4 and 164.0 ppm are attributable respectively to CH_3, CH_2, and COH units of DEF molecule. Signals at $\delta = 137.8$, and 174.5 ppm can be assigned to the carbons of the aromatic and carboxylic functions of terephthalate species respectively.

3.3. Thermogravimetric analysis

The thermogravimetric analysis of $Zn_3(OH)_2(bdc)_2 \cdot 2DEF$ (under N_2, 3 °C min^{-1}, TA Instrument 2050) shows two main events (Fig. 6). The first weight loss (obs: 26.4%), between 110 and 290 °C, could be assigned to the removal of the DEF molecules (calc: 26.6%) occluded within the tunnels of the structure. The second weight loss starts from 290 °C and corresponds to 41.0% at 470 °C. It could be attributed to the departure of the 1,4-benzenedicarboxylate species (calc: 41.3%). At 600 °C, the XRD pattern of the residue

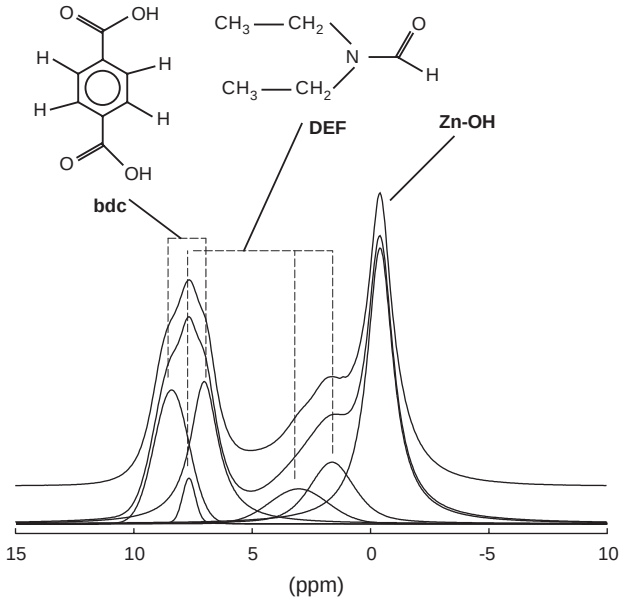

Fig. 7. Experimental ^{1}H MAS NMR spectrum (top) of $Zn_3(OH)_2(bdc)_2 \cdot 2DEF$ collected at a spinning speed of 30 kHz. The simulated spectrum and its decomposition are included (below).

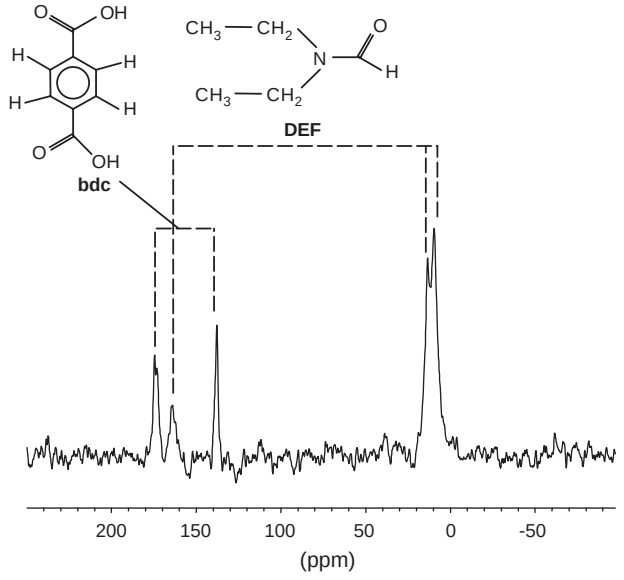

Fig. 8. $^{13}C\{^{1}H\}$ decoupled MAS spectrum of $Zn_3(OH)_2(bdc)_2 \cdot 2DEF$ acquired at a spinning speed of 12.5 kHz.

corresponds to the zinc oxide ZnO. A sample of $Zn_3(OH)_2(bdc)_2 \cdot 2DEF$ was calcined in air at 230 °C to evacuate the pore space, but removal of the DEF molecules resulted in the collapse of the 3D framework. This might be due to the existence of strong hydrogen interactions occurring between the trapped organic species within the structure pores and the μ_3-hydroxy groups of the infinite Zn–O–C chains. Such thermal behavior was previously encountered in the fluorinated gallium phosphates [32], for which strong hydrogen interactions are present between the bridging fluorine atoms belonging to the inorganic $GaPO_4$ framework and the ammonium groups of occluded structure-directing agent molecules. As reported in the recent study about the MOF-69 [11] series, attempts of molecular exchange were tested at room temperature. For instance, in $Zn_3(OH)_2(bdc)_2 \cdot 2DEF$, the occluded DEF species were fully replaced by the tetrahydrofuran ones after immersion of the as-synthesized product overnight.

4. Conclusions

The present study has reported the solvothermal synthesis of a new zinc terephthalate $Zn_3(OH)_2(bdc)_2 \cdot 2DEF$, obtained in the presence of the DEF solvent. This solid possesses a three-dimensional zinc-bdc framework, which encapsulates the DEF species. It is built up from the connection of terephthalate ligands with infinite straight chains of $ZnO_4(OH)_2$ octahedra and bi-tetrahedral $ZnO_2(OH)_2$ units in a strict alternation. This phase is another example of zinc carboxylate networks based on the linkage of bdc moieties with the Zn–O–C cores. By using *N,N′*-dimethylformamide molecules as main solvent, other zinc terephthalates were observed with diverse building motifs. They are described from discrete molecular building blocks consisting of isolated tetrahedra ZnO_4 [33–35] or trigonal bipyramids ZnO_5 [33], trimeric units of one central ZnO_6 octahedron linked to two tetrahedra ZnO_4 [33] or two trigonal bipyramids ZnO_5 [36]. The structures of these zinc-organic networks are rather dense in contrast with those described from other discrete building blocks having higher symmetry. Such more open frameworks are encountered in the compounds containing dimers of square pyramidal species ZnO_5 with a paddle-wheel configuration [37–39], in which four bridging carboxylate groups are arranged in a square. This typical dimeric metal–oxygen motif is also a common feature in the copper(II) carboxylates family [40,41]. The other building block, corresponding to the tetranuclear supertetrahedral unit is observed in the large pore framework MOF-5 [20] and related compounds [21], and is more specific to the crystal-chemistry of zinc. It is composed of a Zn_4O core consisting of a central μ_4-oxo anion bridging four tetrahedrally coordinated zinc atoms. Such an entity was also reported in the zinc phosphates [42,43]. The different phases were synthesized by using various co-solvent molecules such as chlorobenzene, toluene, methanol, etc. The choice of this additional organic species, acting as structure-directing agent, could be an influent parameter for the formation of metal-organic networks with a specific geometry of the Zn–O–C core. This shows the structural

variety and richness of the crystal-chemistry of such systems, which allows for the design and synthesis of novel three-dimensional architectures.

Appendix A. Supplementary data

The online version of this article contains additional supplementary data. Please visit doi:10.1016/j.jssc.2004.08.007.

References

[1] S.R. Batten, R. Robson, Angew. Chem. Int. Ed. 37 (1998) 1460.
[2] P.J. Hagrman, D. Hagrman, J. Zubieta, Angew. Chem. Int. Ed. 38 (1999) 2638.
[3] B. Moulton, M.J. Zaworotko, Chem. Rev. 101 (2001) 1629.
[4] C. Janiak, Dalton Trans. (2003) 2781.
[5] S.L. James, Chem. Soc. Rev. 32 (2003) 276.
[6] O.M. Yaghi, M. O'Keeffe, N.W. Ockwig, H.K. Chae, M. Eddaoudi, J. Kim, Nature 423 (2003) 705.
[7] M.J. Rosseinsky, Microporous Mesoporous Mater. 73 (2004) 15.
[8] G. Férey, Chem. Mater. 13 (2001) 3084.
[9] K. Barthelet, J. Marrot, D. Riou, G. Férey, Angew. Chem. Int. Ed. 41 (2002) 281.
[10] C. Serre, F. Millange, C. Thouvenot, M. Nogues, G. Marsolier, D. Louër, G. Férey, J. Am. Chem. Soc. 124 (2002) 13519.
[11] N.L. Rosi, M. Eddaoudi, J. Kim, M. O'Keeffe, O.M. Yaghi, Angew. Chem., Int. Ed. 41 (2002) 284.
[12] K. Barthelet, J. Marrot, G. Férey, D. Riou, Chem. Commun. (2004) 520.
[13] T. Loiseau, C. Serre, C. Huguenard, G. Fink, F. Taulelle, M. Henry, T. Bataille, G. Férey, Chem. Eur. J. 10 (2004) 1373.
[14] T. Loiseau, C. Mellot-Draznieks, H. Muguerra, G. Férey, M. Haouas, F. Taulelle, Comptes Rendus Chimie (2005) in press.
[15] S. Kitagawa, R. Kitaura, S.-I. Noro, Angew. Chem. Int. Ed. 43 (2004) 2334.
[16] N.L. Rosi, J. Eckert, M. Eddaoudi, D.T. Vodak, J. Kim, M. O'Keeffe, O.M. Yaghi, Science 300 (2003) 1127.
[17] G. Férey, M. Latroche, C. Serre, F. Millange, T. Loiseau, A. Percheron-Guégan, Chem. Commun. (2003) 2976.
[18] L. Pan, M.B. Sander, X. Huang, J. Li, M. Smith, E. Bittner, B. Bockrath, J.K. Johnson, J. Am. Chem. Soc. 126 (2004) 1308.
[19] J.L.C. Rowsell, A.R. Millward, K.S. Park, O.M. Yaghi, J. Am. Chem. Soc. 126 (2004) 5666.
[20] H. Li, M. Eddaoudi, M. O'Keeffe, O.M. Yaghi, Science 402 (1999) 276.
[21] M. Eddaoudi, J. Kim, N. Rosi, D. Vodak, J. Wachter, M. O'Keeffe, O.M. Yaghi, Science 295 (2002) 469.
[22] G.M. Sheldrick, SADABS, a program for the Siemens Area Detector ABSorption correction, 1995.
[23] G.M. Sheldrick, SHELXTL version 5.03, software package for the crystal structure determination, 1994.
[24] N.E. Brese, M. O'Keeffe, Acta Crystallogr. B 47 (1991) 192.
[25] J.S. Seo, D. Whang, H. Lee, S.I. Jun, J. Oh, Y.J. Jeon, K. Kim, Nature 404 (2000) 982.
[26] J. Tao, M.-L. Tong, J.-X. Shi, X.-M. Chen, S.W. Ng, Chem. Commun. (2000) 2043.
[27] J. Hermann, A. Erxleben, Inorg. Chim. Acta 304 (2000) 125.
[28] W. Clegg, D.R. Harbron, C.D. Homan, P.A. Hunt, I.R. Little, B.P. Straughan, Inorg. Chim. Acta 186 (1991) 51.
[29] G.B. Deacon, R.J. Phillips, Coord. Chem. Rev. 33 (1980) 227.
[30] R.L. Rardin, W.B. Tolman, S.J. Lippard, New J. Chem. 15 (1991) 417.
[31] M. O'Keeffe, M. Eddaoudi, H. Li, T.M. Reineke, O.M. Yaghi, J. Solid State Chem. 152 (2000) 3.
[32] L. Beitone, J. Marrot, T. Loiseau, G. Férey, M. Henry, C. Huguenard, A. Gansmüller, F. Taulelle, J. Am. Chem. Soc. 125 (2003) 1912.
[33] M. Edgar, R. Mitchell, A.M.Z. Slawin, P. Lightfoot, P.A. Wright, Chem. Eur. J. 7 (2001) 5168.
[34] S.-Y. Yang, Z.-G. Sun, L.-S. Long, R.-B. Huang, L.-S. Zheng, Main Group Met. Chem. 25 (2002) 579.
[35] L.-N. Zhu, L.Z. Zhang, W.-Z. Wang, D.-Z. Liao, P. Cheng, Z.-H. Jiang, S.-P. Yan, Inorg. Chem. Commun. 5 (2002) 1017.
[36] H. Li, C.E. Davis, T.L. Groy, D.G. Kelley, O.M. Yaghi, J. Am. Chem. Soc. 120 (1998) 2186.
[37] H. Li, M. Eddaoudi, T.L. Groy, O.M. Yaghi, J. Am. Chem. Soc. 120 (1998) 8571.
[38] D.N. Dybtsev, H. Chen, K. Kim, Angew. Chem., Int. Ed. 43 (2004) 5033.
[39] M. Eddaoudi, J. Kim, J.B. Wachter, H.K. Chae, M. O'Keeffe, O.M. Yaghi, J. Am. Chem. Soc. 123 (2001) 4368.
[40] S.M.-F. Lo, S.S.-Y. Chui, L.-Y. Shek, Z. Lin, X.X. Zhang, G.-H. Wen, I.D. Williams, J. Am. Chem. Soc. 122 (2000) 6293.
[41] W. Mori, S. Takamizawa, J. Solid State Chem. 152 (2000) 120.
[42] W.T.A. Harrison, R.W. Broach, R.A. Bedard, T.E. Gier, X. Bu, G.D. Stucky, Chem. Mater. 8 (1996) 691.
[43] W.T.A. Harrison, M.L.F. Phillips, A.V. Chavez, T.M. Nenoff, J. Mater. Chem. 9 (1999) 3087.